Earth Planet. Sci. Lett. 641 (2024) 118768

Contents lists available at ScienceDirect

Earth and Planetary Science Letters

journal homepage: www.elsevier.com/locate/epsl

Highly siderophile element evidence for mantle plume involvement during opening of the Atlantic Ocean

James M.D. Day [a,*], Sarah J. Woodland [b], Kimberley L. Nutt [a], Nicole Stroncik [c], Lotte M. Larsen [d], Robert B. Trumbull [c], D. Graham Pearson [b]

[a] Geosciences Research Division, Scripps Institution of Oceanography, La Jolla, CA 92093-0244, USA
[b] Department of Earth and Atmospheric Sciences, University of Alberta, Edmonton, Alberta, T6G 2E3, Canada
[c] Helmholtz Centre Potsdam GFZ German Research Centre for Geosciences, Telegrafenberg, Potsdam, Germany
[d] Geological Survey of Denmark and Greenland (GEUS), Øster Voldgade 10 DK-1350 Copenhagen K, Denmark

ARTICLE INFO

Editor: Dr C. M. Petrone

Keywords:
Continental flood basalts
Highly siderophile elements
Os isotopes
High $^{3}He/^{4}He$
Continental break-up

ABSTRACT

Osmium isotope and highly siderophile element (HSE: Os, Ir, Ru, Pt, Pd, Re) abundance data are reported for picrites and basalts from the ~132 Ma Etendeka large igneous province (LIP) and the ~60 Ma North Atlantic Igneous Province (NAIP). Picrite dykes of the Etendeka LIP have HSE abundances and $^{187}Os/^{188}Os$ (0.1276 to 0.1323; γOs_i = -0.5 to +3.1) consistent with derivation from high-degree partial melting (>20 %) of a peridotite source with chondritic to modestly supra-chondritic long-term Re/Os. High-$^{3}He/^{4}He$ NAIP picrites from West Greenland represent large-degree partial melts with similarly elevated HSE abundances and $^{187}Os/^{188}Os$ (0.1273 to 0.1332; γOs_i = -0.2 to +3.9). Broadly chondritic Os isotope ratios have also been reported for the ~132 Ma Paraná LIP and the ~201 Ma Central Atlantic Magmatic Province (CAMP). Consequently, LIP associated with Atlantic Ocean opening derive, at least in part, from partial melting of peridotite mantle distinct from the depleted mantle associated with mid-ocean ridge basalt volcanism. Modern locations with high-$^{3}He/^{4}He$ (>25R_A) include ocean island basalts (OIB) from Ofu (Samoa), Loihi (Hawaii) and Fernandina (Galapagos) in the Pacific Ocean, and from Iceland, which is considered the modern manifestation of NAIP magmatism. Unlike Etendeka and NAIP picrites, these modern OIB have Sr-Nd-Pb-Os isotopes consistent with contributions of recycled oceanic or continental crust. The lower degree of partial melting responsible for modern high-$^{3}He/^{4}He$ OIB gives higher proportions of fusible recycled crustal components to the magmas, with radiogenic $^{187}Os/^{188}Os$ and low-$^{3}He/^{4}He$. The high-$^{3}He/^{4}He$, incompatible trace element-depleted mantle component in both LIP and OIB therefore also has long-term chondritic Re/Os, which is consistent with an early-formed reservoir that experienced late accretion. Atlantic LIP (CAMP; Paraná-Etendeka; NAIP) provide geochemical evidence for a prominent role for mantle plume contributions during continental break-up and formation of the Atlantic Ocean, a feature hitherto unrecognized in other ocean basin-forming events.

1. Introduction

Continental break-up that forms new ocean basins is an integral feature of plate tectonics, and a fundamental process in supercontinent disassembly (e.g., Storey, 1995). Whether continental break-up occurs through *passive* rifting from far-field tectonic forces or thermal incubation under supercontinents (e.g., Lu and Huismans, 2021), or through *active* rifting, driven by forceful penetration of the lithosphere by mantle plumes (e.g., Courtillot et al., 1999), however, remains debated. Opening of the Atlantic Ocean from the Triassic to the Paleogene is the most recent large-scale ocean basin-forming event and its comparatively good state of preservation offers the chance to assess the role that plume-driven processes might play in continental break-up. The Atlantic Ocean is associated with three voluminous large igneous provinces (LIP), the ~201 Ma Central Atlantic Magmatic Province that is preserved at localities in North America, South America, West Africa and across the Iberian Peninsula (CAMP; e.g., Whalen et al., 2015), the ~132 Ma Paraná-Etendeka LIP of Brazil and Namibia (e.g., Renne et al., 1996), and the ~60 Ma North Atlantic Igneous Province, extending from Arctic Canada to Greenland and to the British Isles (NAIP; e.g., Saunders et al.,

* Corresponding author.
E-mail address: jmdday@ucsd.edu (J.M.D. Day).

https://doi.org/10.1016/j.epsl.2024.118768
Received 31 October 2023; Received in revised form 4 May 2024; Accepted 11 May 2024
Available online 11 June 2024

1997) (Fig. 1).

There are petrological arguments for both anomalously high mantle potential temperatures for Atlantic LIP (e.g., Larsen and Pedersen, 2000), and temperatures similar to, or marginally higher than ambient mantle values (e.g., Buiter and Torsvik, 2014; Prasanth et al., 2022). Geochemically, the mantle sources of magmatism for Atlantic LIP can be challenging to constrain, because of crustal contamination and fractional crystallization processes acting on even the most primitive parent magmas (e.g., Thompson et al., 2001; Day, 2016). However, both the NAIP and Paraná-Etendeka LIP contain picrites with near primary compositions, suggesting anomalously high degrees of partial melting (e.g., Thompson and Gibson, 2000; Larsen and Pedersen, 2009). Picrites from these locations can have high-^{3}He/^{4}He ratios (reported as R_A, or the ^{3}He/^{4}He ratio of air, 1.38×10^{-6}), characteristic of less-degassed mantle sources than the depleted mid-ocean ridge basalt mantle (DM) (Graham et al., 1998; Stuart et al., 2003; Starkey et al., 2009; Stroncik et al., 2017). This provides geochemical evidence for mantle contributions akin to modern-day high-^{3}He/^{4}He ocean island basalts (OIB) (e.g., Kurz et al., 1982; Valbracht et al., 1997; Hilton et al., 1999; Day et al., 2022a). The Sr-Nd-Pb isotope signatures of the most primitive picrites are also consistent with originating from a long-term incompatible trace-element depleted mantle source that is also observed in high-^{3}He/^{4}He OIB (e.g., Hart et al., 1992).

In this study, we report new Re-Os isotope and highly siderophile element (HSE: Os, Ir, Ru, Pt, Pd, Re) abundance data for samples from the 132 Ma Etendeka Province, and HSE data for the ~60 Ma West Greenland picrites (NAIP). The HSE abundances and ratios, and the Re-Os isotope system embedded within them, are powerful tools for understanding crustal and lithospheric contributions to basaltic lavas, and for examining prevalent mantle source compositions (e.g., Carlson, 2005; Day, 2013). Early erupted and primitive picrites are particularly useful for examining major source components involved during mantle melting. Specifically, Os isotope data for the most primitive LIP lavas have been crucial for assessing the role of crustal contamination, melt-depleted mantle source reservoirs like DM or Archaean cratonic continental lithospheric mantle, or less-depleted mantle contributions (e.g., Ellam et al., 1992; Horan et al., 1995; Schaefer et al., 2000; Dale et al., 2009; Li et al., 2010; Day et al., 2013; 2021; Heinonen et al., 2014; Peters and Day, 2017). The relationship between high-^{3}He/^{4}He melts associated with the opening of the Atlantic Ocean and other high-^{3}He/^{4}He products from modern OIB both in the Atlantic (Iceland) and Pacific (Loihi, Hawaii; Ofu, Samoa; Fernandina, Galapagos) are also explored to understand the likely extent of mantle contributions versus recycled crustal components in their sources.

2. Samples and methods

Osmium isotope and highly siderophile element (HSE) abundance data were determined on Etendeka samples that were previously studied for He-Sr-Nd-Pb isotopes (Stroncik et al., 2017). Additionally, HSE abundances are reported for high-^{3}He/^{4}He West Greenland samples for which He-Sr-Nd-Os-Pb isotope data already exist (Graham et al., 1998; Larsen and Pedersen, 2009; Starkey et al., 2009; Dale et al., 2009). Bulk rock trace-element abundances were determined on Etendeka and West Greenland sample powders prior to Os isotope and HSE abundance analyses. Etendeka sample analyses were performed at Scripps Institution of Oceanography and the West Greenland samples were measured at Durham University, UK. Both HSE abundance and Os isotope datasets were obtained using similar isotope dilution Carius tube methodologies and with similar precision and accuracy, demonstrated by analysis of the HARZ-01 and GP13 standard reference materials prepared with the samples (*Table S1*). Detailed methods are given in the *Supplementary Information* (including new trace element abundance data presented in *Table S2*).

3. Results

Major-, minor- and trace-element abundance data, and He-(O)-Sr-Nd-Pb isotope ratios have been reported for the Etendeka and West Greenland samples studied here (Larsen and Pedersen, 2009; Starkey et al., 2009; Stroncik et al., 2017). Helium isotope data for West Greenland olivine separates were obtained by crushing *in vacuo*, whereas for Etendeka olivine separates, He isotope data were obtained on samples shielded from cosmogenic ray exposure and using a stepped heating technique. We treat the data from these techniques without prejudice, although stepped heating may release lattice-bound ^{4}He, or cosmogenically produced ^{3}He, if present. Any cosmogenically produced ^{3}He would increase the ^{3}He/^{4}He ratio measured in samples. Future *in*

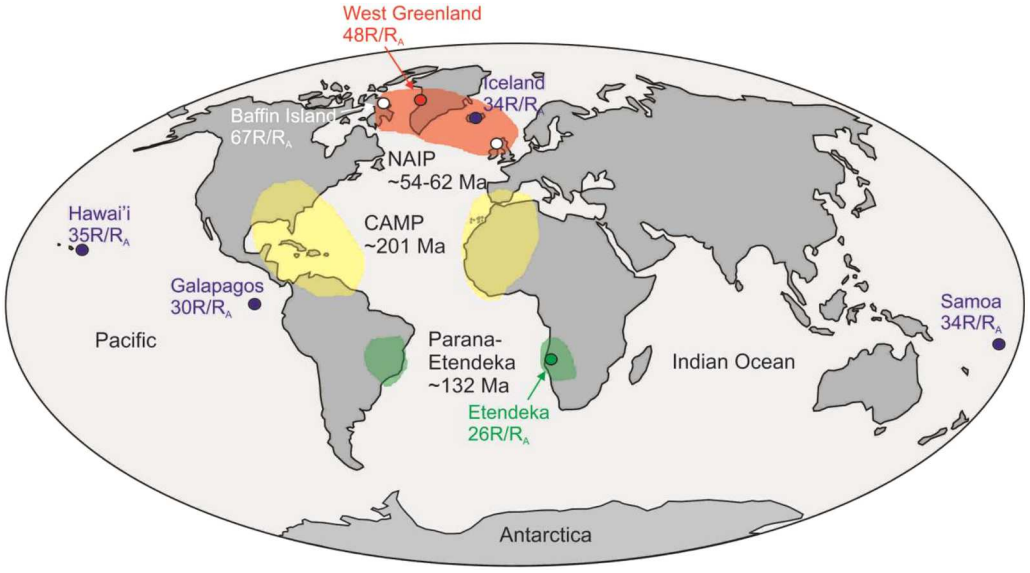

Fig. 1. Sketch Map of the Earth centered on the Atlantic Ocean basin showing the relationship of the ~201 Ma Central Atlantic Magmatic Province (CAMP; yellow shaded regions), ~132 Ma Parana-Etendeka large igneous province (green shaded regions) and ~54–62 Ma North Atlantic Igneous Province (NAIP; red shaded region). Also shown are maximum high-^{3}He/^{4}He ratios for NAIP lavas (Baffin Island, West Greenland), Etendeka samples and modern ocean island basalts with maximum ^{3}He/^{4}He of 30R_A or greater. Helium isotope data from Valbracht et al. (1997); Graham et al. (1998); Stuart et al. (2003); Macpherson et al. (2005); Jackson et al. (2009); Kurz et al. (2009); Starkey et al. (2009); Stroncik et al. (2017); Horton et al. (2023).

vacuo crushing of Etendeka picrite olivine will therefore be important for confirming intrinsic high-$^3He/^4He$ in these samples. Northern Etendeka samples (from <21°S) were collected from basaltic to picritic dykes and basal lava flows (8.5 to 19.6 wt. % MgO). They have mantle-like $\delta^{18}O_{olivine}$ (5.3 to 5.7 ‰), elevated incompatible trace element abundances (*Figure S1*), variable age-corrected $^{87}Sr/^{86}Sr$ (0.70489 to 0.70792) and $^{143}Nd/^{144}Nd$ (0.51293 to 0.51264), and Pb isotope ratios plotting above the northern hemisphere reference line (NHRL) (Fig. 2); some also have high-$^3He/^4He$ (up to ~26R_A; Stroncik et al., 2017). Southern Etendeka samples (from >21°S) were collected from picritic dykes (13.9 to 21.8 wt. % MgO) intruding Neoproterozoic metasediments. These have mantle-like to high $\delta^{18}O_{olivine}$ (5.8 to 6.4‰) and generally lower absolute incompatible trace element abundances than northern Etendeka samples (*Figure S1*). They have higher age-corrected $^{87}Sr/^{86}Sr$ (0.70714 to 0.70883) and lower $^{143}Nd/^{144}Nd$ (0.51257 to 0.51248), with Pb isotope ratios plotting above the NHRL and to the right of the geochron (Fig. 2). Some also have high-$^3He/^4He$ (up to ~21R_A; Stroncik et al., 2017).

West Greenland samples are from three distinct lithological members (Anaanaa, Naujánguit, Ordlingassoq) and are generally tholeiitic picrites (17.3 to 26.3 wt. % MgO) with high-$^3He/^4He$ ratios (up to ~48R_A; Starkey et al., 2009; Larsen and Pedersen, 2009). Age-corrected $^{87}Sr/^{86}Sr$ (0.70298 to 0.70468) and $^{143}Nd/^{144}Nd$ (0.51311 to 0.51276), as well as unradiogenic Pb isotope ratios close to the geochron and at or below the NHRL, suggest that the studied samples were negligibly contaminated by crust (Larsen and Pedersen, 2009; Fig. 2).

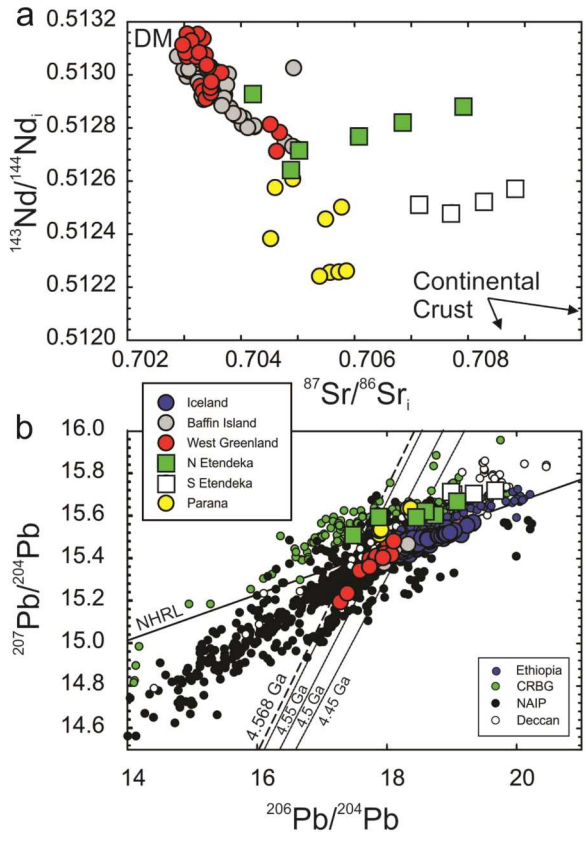

Fig. 2. Age corrected (a) $^{87}Sr/^{86}Sr$ versus $^{143}Nd/^{144}Nd$ for ~132 Ma Paraná-Etendeka LIP and ~60 Ma Baffin Island and West Greenland picrites. (b) $^{206}Pb/^{204}Pb$ versus $^{207}Pb/^{204}Pb$ for Iceland picrites and other LIP. Data for (a) are given in Table 1 or are from Starkey et al. (2009) and Rocha-Junior et al. (2012). Shown in (a) are the general distributions for depleted mantle (DM) and continental crust reservoirs based on Day (2016). Data in (b) from the same sources with additional data for Ethiopia, Deccan, Columbia River Basalt Group (CRBG), and North Atlantic Igneous Province (NAIP) compiled in Day (2016). NHRL = Northern Hemisphere Reference Line and geochrons shown for different times, up to 4.45 Ga.

Osmium isotope and HSE abundance data for Etendeka and West Greenland picrites and basalts are reported in Table 1. Northern Etendeka samples have variable Os contents (0.26 to 3.6 ng/g) and fractionated primitive mantle (PM) normalized HSE (Re, Pd, Pt, Ru, Ir, Os) patterns, as well as variable $^{187}Re/^{188}Os$ (0.8 to 24) and $^{187}Os/^{188}Os$ (0.1317 to 0.1831) ratios that suggest the basaltic samples experienced more extensive fractional crystallization than picrites (Figs. 3, 4, 5). Age-corrected Os isotope compositions, expressed as γOs_i (where γOs_i is the percentage deviation in $^{187}Os/^{188}Os$ relative to a chondritic reference calculated for a specified time), span a limited range from +0.2 to +5. Southern Etendeka picrites have higher Os contents (2.2 to 4.2 ng/g), less-fractionated PM-normalized HSE patterns, as well as lower and less variable $^{187}Re/^{188}Os$ (0.2 to 0.7) and $^{187}Os/^{188}Os$ (0.1276 to 0.1294) ratios, with γOs_i from −0.5 to +1.8 (Figs. 3, 4, 5). Thompson et al. (2007) reported Re-Os isotope data for olivine separates from two southern Etendeka dykes ($^{187}Os/^{188}Os$ = 0.126 to 0.130; γOs_i = −2 to −0.4) that are similar to the bulk rock data for southern Etendeka samples provided here.

Rhenium-osmium isotope data for the West Greenland picrites analysed for HSE abundances here, were reported by Dale et al. (2009). These samples have high Os contents (1.5 to 3.9 ng/g), a range in $^{187}Re/^{188}Os$ (0.14 to 2.17), $^{187}Os/^{188}Os$ (0.1273 to 0.1332) and γOs_i (−0.2 to +3.9) (Figs. 3 and 5). The concentrations of Pd, Pt, Ru and Ir in these samples, as well as the PM-normalized HSE patterns are similar to those of the highest-MgO picrites from the Etendeka LIP province (Fig. 4). Collectively, the HSE patterns for samples from both Etendeka and West Greenland are some of the most primitive of all LIP studied to date.

4. Discussion

4.1. Primary mantle source compositions for Paraná-Etendeka LIP

The reported Re-Os isotope and HSE abundance data for Etendeka picrites complement a study of basalts from the associated Paraná LIP of Brazil (Rocha-Junior et al., 2012). The HSE contents of Paraná-Etendeka lavas vary as a function of MgO content, and lower MgO samples from this study (e.g., N. Etendeka) have similarly fractionated PM normalized patterns with high (Pd+Pt)/(Os+Ir+Ru). The Paraná basalts (4.8–7.1 wt. % MgO) have near-chondritic Os isotope compositions and low $^{143}Nd/^{144}Nd$, with the latter suggestive of crustal assimilation (Fig. 2). Etendeka picrites and basalts have incompatible lithophile element and Sr-Nd-Pb isotope compositions (Fig. 2), consistent with variable assimilation of Neoproterozoic metasediments, concomitant with fractional crystallization (e.g., Thompson et al., 2001; 2007; Stroncik et al., 2017). Despite evidence for crustal assimilation from lithophile radiogenic isotopes, a remarkable feature of the Etendeka – and Paraná – LIP is the limited range in initial $^{187}Os/^{188}Os$ (γOs_i; +2 ± 1.7 [1 St Dev]) ratios across a wide range of Os contents (Fig. 3). This average value is marginally supra-chondritic, similar to the estimated γOs value for PM (+1.6; e.g., Day et al., 2017) and highly distinct from depleted, low Re/Os cratonic continental lithospheric mantle (CLM, e.g., γOs <0; e.g., Pearson et al., 2004).

Studies of Etendeka picrites have shown that their parental magmas had at least ~>13.5 wt. % MgO and may have had as much as 20 wt. % MgO (e.g., Thompson and Gibson, 2000), equating to >20 % partial melting, also consistent with rare earth element modelling (*Supplementary Information*). Initiation of melting occurred from 180 to 120 km at mantle potential temperatures estimated between 1325 to >1500 °C, or possibly as high as 1700 °C (e.g., Thompson et al., 2001; Cheng et al., 2019; Prasanth et al., 2022).

Models to explain HSE abundances in LIP have been developed to explain both partial melt compositions and later effects of fractional crystallization. For example, both the Miocene Columbia River Basalt Group (Western USA; Day et al., 2021) and basalts from the Proterozoic

Table 1
Rhenium-osmium isotopes and highly siderophile element abundances (in ng/g) for Etendeka and West Greenland picrites and basalts with He-Sr-Nd-Pb isotope data.

Sample	Lab	Group	Member	MgO (wt.%)	Os	Ir	Ru	Pt	Pd	Re	$^{187}Re/^{188}Os$	±2SD	$^{187}Os/^{188}Os$	±2SE	$^{187}Os/^{188}Os_i$	γOs_i	$^{3}He/^{4}He$ (R/R_A)	$^{87}Sr/^{86}Sr$	$^{143}Nd/^{144}Nd$	$^{206}Pb/^{204}Pb$
Etendeka Picrites and Basalts (132 Ma)																				
KT-10-8	SIGL	N	Twyfelfontein	12.8	0.78	0.55	0.60	7.59	2.92	0.484	3.000	0.045	0.13781	0.00015	0.1312	3.6	*3.1*	*0.70501*	*0.51272*	*18.42*
KT-10-9	SIGL	N	Twyfelfontein	12.4	2.66	1.59	2.61	13.11	11.91	0.504	0.914	0.014	0.13514	0.00009	0.1331	5.1	*2.7*	*0.70489*	*0.51264*	*17.48*
KT-10-5	SIGL	N	Doros	8.5	0.26	0.18	0.33	9.38	15.45	0.627	11.58	0.174	0.15803	0.00017	0.1325	4.6	*13.0*	*0.70607*	*0.51277*	*19.08*
KT-10-6	SIGL	N	Doros	12.6	0.29	0.32	0.33	3.86	3.12	1.447	24.10	0.361	0.18314	0.00030	0.1301	2.7				
KT-10-7	SIGL	N	Doros	11.1	0.77	0.49	0.97	16.40	16.58	0.544	3.424	0.051	0.13719	0.00017	0.1297	2.3	*9.6*	*0.70421*	*0.51293*	*18.73*
KT-10-2	SIGL	N	Brandberg	19.6	3.57	2.02	2.45	9.45	10.90	0.573	0.775	0.012	0.13232	0.00009	0.1306	3.1	*3.8*	*0.70685*	*0.51282*	*18.57*
KT-10-3	SIGL	N	Brandberg	19.5	1.91	1.21	2.93	11.75	7.93	0.843	2.133	0.032	0.13167	0.00009	0.1270	0.2	*25.9*	*0.70792*	*0.51288*	*17.88*
KT-10-1	SIGL	S	Spitzkoppe	21.8	3.43	1.88	3.83	7.94	6.56	0.385	0.541	0.008	0.12794	0.00009	0.1267	0.0	*5.8*	*0.70883*	*0.51257*	*19.67*
Rpt	SIGL			21.8	3.27	1.97	3.88	4.80	5.95	0.154	0.227	0.003	0.12930	0.00020	0.1288	1.7				
KT-10-10	SIGL	S	Spitzkoppe	17.3	2.23	1.20	2.72	8.27	4.40	0.317	0.686	0.010	0.12757	0.00009	0.1261	-0.5	*1.8*	*0.70828*	*0.51252*	*19.34*
KT-10-11	SIGL	S	Spitzkoppe	13.9	2.31	1.67	1.77	5.78	6.59	0.327	0.682	0.010	0.12879	0.00011	0.1273	0.5	*21.0*	*0.70714*	*0.51251*	*19.00*
Q15	SIGL	S	Spitzkoppe	19.4	4.20	2.60	4.39	7.56	6.33	0.172	0.197	0.003	0.12942	0.00007	0.1290	1.8				
Q22	SIGL	S	Spitzkoppe	15.3	2.28	1.35	1.89	5.81	6.34	0.241	0.509	0.008	0.12905	0.00010	0.1279	1.0	*1.2*	*0.70771*	*0.51248*	*19.03*
West Greenland Picrites (60 Ma)																				
GGU400444	DU		Anaanaa	20.1	*1.91*	0.94	2.63	7.48	6.97	*0.259*	0.655	0.010	*0.12812*	*0.00008*	*0.1275*	0.2		*0.70468*	*0.51278*	*17.28*
GGU400457	DU		Anaanaa	21.7	*3.88*	1.94	3.61	11.16	9.35	*0.359*	0.446	0.007	*0.12765*	*0.00005*	*0.1272*	0.0	*17.6*	*0.70334*	*0.51314*	*17.81*
GGU400492	DU		Anaanaa	19.3	*2.53*	1.33	3.26	10.69	10.30	*1.140*	2.170	0.033	*0.13024*	*0.00007*	*0.1281*	0.7		*0.70324*	*0.51315*	*17.84*
GGU408001.233	DU		Anaanaa	18.8	*1.50*	0.80	2.99	9.53	8.74	*0.243*	0.779	0.012	*0.12824*	*0.00010*	*0.1275*	0.2		*0.70452*	*0.51281*	*17.39*
GGU113210	DU		Naujánguit	20.9	*3.12*	1.64	4.41	13.00	10.90	*0.206*	0.318	0.005	*0.12725*	*0.00006*	*0.1269*	-0.2		*0.70322*	*0.51307*	*17.58*
GGU264217	DU		Naujánguit	21.2	*2.79*	1.48	4.26	11.42	11.58	*0.472*	0.815	0.012	*0.12772*	*0.00008*	*0.1269*	-0.2	*19.1*	*0.70305*	*0.51315*	*18.02*
Rpt	DU				*2.79*	1.46	4.48	11.44	11.50	0.461	0.783	0.012								
GGU332771	DU		Naujánguit	19.3	*1.55*	0.93	3.00	9.59	10.95	*0.425*	1.319	0.020	*0.12837*	*0.00009*	*0.1271*	-0.1		*0.70313*	*0.51313*	*17.73*
GGU362149	DU		Naujánguit	23.7	*2.81*	1.58	3.91	9.95	8.57	*0.291*	0.499	0.007	*0.12814*	*0.00008*	*0.1276*	0.4	*30.7*	*0.70303*	*0.51308*	*17.96*
Rpt	DU				*2.72*	1.49	3.66	9.90	8.74	0.286	0.498	0.007								
GGU113333	DU		Ordlingassoq	20.6	*2.26*	1.19	3.31	9.54	6.66	*0.063*	0.135	0.002	*0.12955*	*0.00007*	*0.1294*	1.8		*0.70327*	*0.51308*	*18.07*
GGU138228	DU		Ordlingassoq	17.3	*1.52*	0.81	2.55	8.76	7.14	*0.330*	1.044	0.016	*0.13321*	*0.00008*	*0.1322*	3.9		*0.70340*	*0.51304*	*18.07*
GGU332788	DU		Ordlingassoq	26.3	*2.03*	1.08	3.14	6.27	4.20	*0.180*	0.427	0.006	*0.13120*	*0.00007*	*0.1308*	2.8	*30.6*	*0.70348*	*0.51297*	*18.11*
Rpt	DU					1.11	2.95	6.01	4.48	0.179										
GGU332828	DU		Ordlingassoq	22.5	*2.68*	1.36	3.20	9.41	6.69	*0.367*	0.660	0.010	*0.13060*	*0.00006*	*0.1299*	2.2	*28.1*	*0.70298*	*0.51311*	*17.94*

Measurements were made at the Scripps Isotope Geochemistry Laboratory (SIGL), and Durham University (DU). Locations, He-O-Sr-Nd-Pb and olivine compositions for Etendeka samples were reported previously in Stroncik et al. (2017). For West Greenland picrites, He isotope data are from Graham et al. (1998), and Starkey et al. (2009) and Sr-Nd-Pb isotope data are reported in Larsen & Pedersen (2009), along with locations. Rhenium and Os isotope data were previously reported in Dale et al. (2009) and these data are shown in italics along with other published data. For the full table, please see the supplementary information. $\gamma Os = ([^{187}Os/^{188}Os_{sample(t)}/^{187}Os/^{188}Os_{chondrite(t)}] -1) \times 100$. Rpt = Complete chemical duplicate measurement of same sample powder. All previously published data shown in italics.

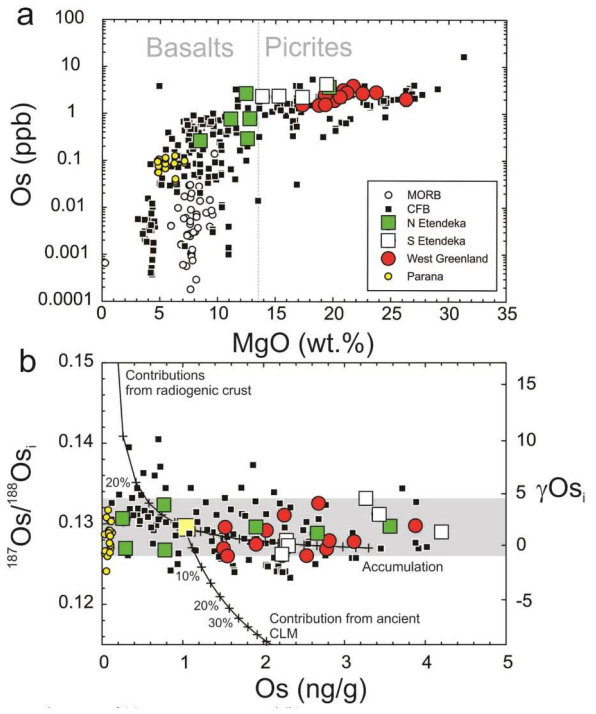

Fig. 3. Diagrams of (a) MgO versus Os and (b) Os versus age-corrected $^{187}Os/^{188}Os$ for Paraná-Etendeka and West Greenland samples versus global continental flood basalts (CFB), showing mixing curves (in 5 % increments) between a model parental melt composition, crust and ancient continental lithospheric mantle and the effect of accumulation of phases with chondritic Os composition. Note the limited range in $^{187}Os/^{188}Os_i$ for a large range in Os content for Etendeka and West Greenland samples (illustrated by the grey field), suggesting limited to no contributions from radiogenic crustal components, which would otherwise change the bulk compositional characteristics of samples. Global compilation of CFB and mixing lines are from Day et al. (2021), with model parameters given in *Table S3*.

Coppermine Volcanics (Canada; Day et al., 2013) have MgO contents typically <8 wt. % and show significant HSE fractionation relative to basaltic lavas from the NAIP, Deccan Traps, Paraná-Etendeka or Karoo-Ferrar LIP, where high MgO basalts and picrites also occur (e.g., Ellam et al., 1992; Schaefer et al., 2000; Stroncik et al., 2017; Peters and Day, 2017). Significant HSE fractionation occurs in melts due to the onset of sulfur saturation, which in OIB occurs at ~8 wt. % MgO, and likely occurs at similar to higher MgO contents for mid-ocean ridge basalts (MORB) (Day, 2013). High sulfide partition coefficients for Os, Ir and Ru relative to Pt and Pd during primitive basaltic magma evolution (e.g., Mungall and Brenan, 2014) leads to strong fractionation. Despite parameter-dependent complexities of melt models (e.g., silicate minerals in the fractionating assemblage, MgO and S content of initial melt, FeS activity and partition coefficients into sulfide), the fractionation behavior of the HSE down to low-MgO lavas are reproduced reasonably well (e.g., Day et al., 2013; 2021), and reinforce a greater degree of HSE fractionation experienced by the northern Etendeka samples that generally also have lower MgO contents than the southern Etendeka samples.

To assess how magmatic processes act on the HSE for the Etendeka LIP, a fractional crystallization model (grey lines) with a partial melting model (red lines) are shown in Fig. 4. The partial melting model produces a primary melt with an assumed value of 20 wt. % MgO from a PM starting composition (~35 wt. % MgO; 250 μg/g S; in ng/g = Os 3.9; Ir 3.5; Ru 7; Pt 7.6; Pd 5.3; Re 0.35; after Day et al., 2017). Fractional crystallization was modelled by removal of olivine coupled with S-saturation in the melt as a function of initial S content and decreasing MgO and, hence, temperature. The models show that the most primitive southern Etendeka picrites have HSE contents broadly consistent with derivation from a source with abundances of the HSE similar to PM. With increasing degrees of fractional crystallization, Ru, Ir and Os behave as strongly compatible elements, scavenged into sulfides or alloys, whereas Pd and Pt behave incompatibly, being enriched in the melt. These fractionations can be reproduced by crystallization of a dominant olivine assemblage (>98 %) with minor sulfide. Linear regression of the Etendeka compositions to the assumed primary melt composition (20 wt. % MgO) gives (in ng/g) Re 0.4; Pd 6.3; Pt 7.7; Ru 3.3; Ir 1.9; Os 3.2. The Etendeka samples, therefore, can be modelled by large-degree partial melting (>20 %) of peridotite with Os isotope and HSE abundance characteristics similar to PM estimates, supported by REE inter-element modelling (*Supplementary Information*).

4.2. Primary mantle source compositions for West Greenland picrites

Rhenium-osmium isotope studies have been conducted on West Greenland tholeiitic picrites (Schaefer et al., 2000; Dale et al., 2009), and ^{187}Re-^{187}Os and HSE abundance data are also available from the rare metalliferous basalts and sedimentary xenoliths that exist within the lava sequence (Pernet-Fisher et al., 2017). The sedimentary xenoliths are characterized by radiogenic $^{187}Os/^{188}Os$ (γOs at ~60 Ma of +145 to +794) and Os-rich metalliferous basalts assimilated this type of crust, with radiogenic Os (γOs at ~60 Ma of +14 to +49; Pernet-Fisher et al., 2017). By contrast, high-MgO volcanic rocks from the Manîtdlat Member of the Vaigat Formation show evidence for incorporation of CLM ($\gamma Os_i = -16$; Larsen et al., 2003), which may also be present in some younger East Greenland lavas (Peate et al., 2003). The West Greenland picrites studied here have all been minimally contaminated by crust or CLM according to previous work (Larsen and Pedersen, 2009; Dale et al., 2009; Starkey et a., 2009). Of the three different members examined in this study (Table 1), the Ordlingassoq Member has the most radiogenic $^{187}Os/^{188}Os$ ($\gamma Os_i = +2.7 \pm 1$) and has been interpreted as possibly containing ~5 % recycled oceanic crust in its mantle source (Dale et al., 2009).

Petrogenetic information from West Greenland picrites suggest that parental magmas were MgO-rich (17–18.5 wt. %) and likely formed by ~16–20 % partial melting initiating at depths of >100 km, and at high mantle potential temperatures (>1520 °C; Larsen and Pedersen, 2000, 2009).

Using the same models employed for the Etendeka, the role of magmatic processes acting on the HSE are assessed for West Greenland picrites in Fig. 4b. The PM-melting model reproduces the overall HSE patterns of the most primitive West Greenland picrites well and, given similar degrees of partial melting for both Etendeka and West Greenland picrites, indicates PM-like characteristics of mantle sources for both localities. Linear regression for West Greenland picrites yields a primary melt composition (at 20 wt. % MgO; in ng/g Re 0.3; Pd 9.2; Pt 10.1; Ru 3.4; Ir 1.2; Os 2.3). These estimates resemble those made by Waterton et al. (2021) for the Ordlingassoq (23 wt. % MgO, in ng/g Pd 5.7; Pt 7.9; Ru 3) and Naujánguit Members (23 wt. % MgO, in ng/g Pd 8.9; Pt 10.4; Ru 4). Notably, the HSE estimates for Greenland are slightly more enriched in Pt and Pd and depleted in Ir than those predicted for Etendeka primary melts. However, the limited range in MgO for the West Greenland picrites (17.3–26.3 wt. % MgO versus 8.5–21.8 wt. % MgO for Etendeka) gives greater uncertainty in the regression calculations for the former.

The HSE patterns of the West Greenland picrites are consistent with limited fractional crystallization and support an origin as primary melts from as much as 20 % partial melting, as confirmed by HSE and REE modelling (Fig. 4 and *Supplementary Information*). As with the Etendeka picrites, these fractionations can be reproduced by crystallization of a dominant olivine assemblage (>98 %) with minor sulfide, but never reach S saturation. Observed variations in $^{187}Os/^{188}Os$ as a function of Os content (Fig. 3) or as a function of $^{187}Re/^{188}Os$ (Fig. 5) can therefore be attributed to initial isotopic source heterogeneity reflected in distinct

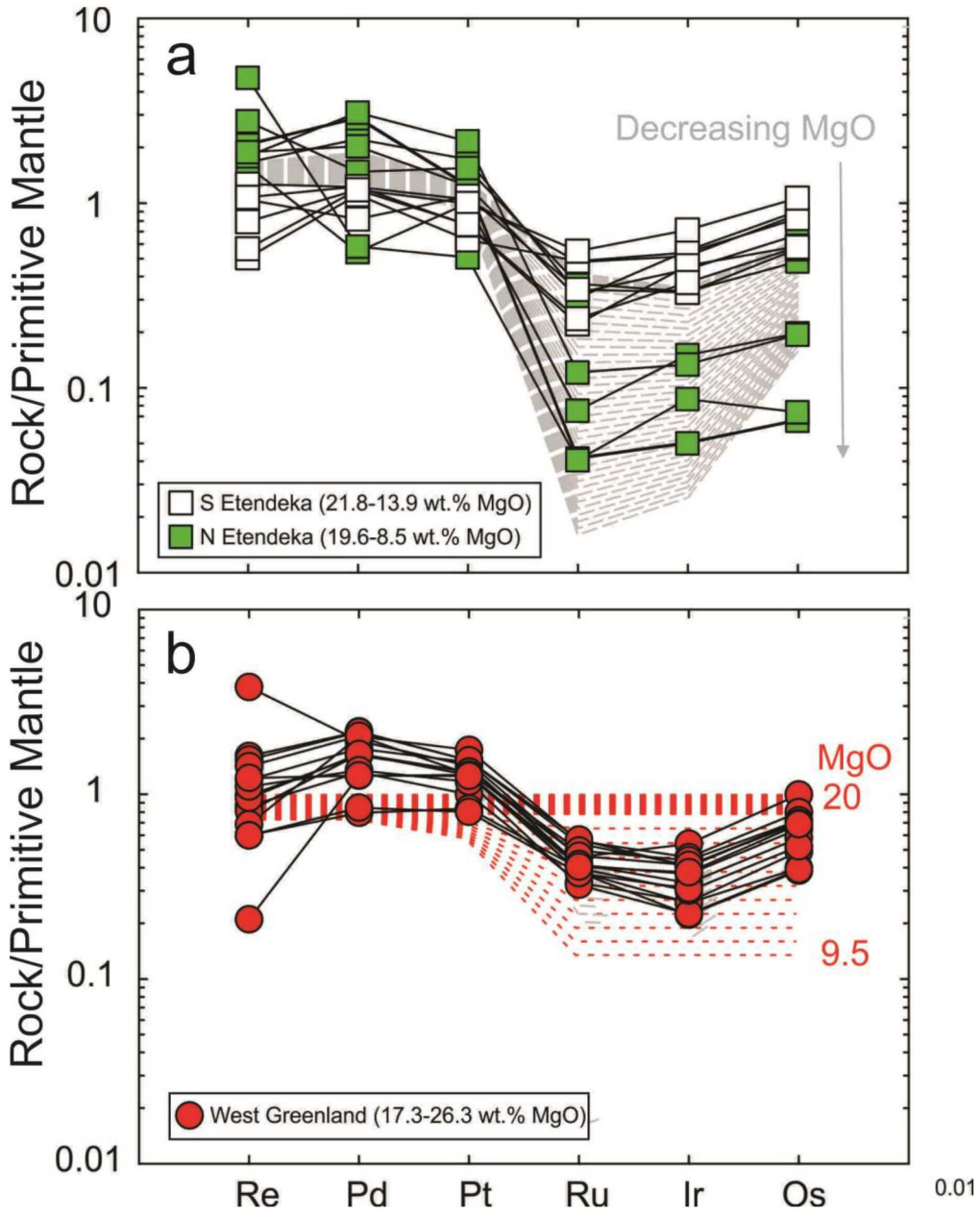

Fig. 4. Highly siderophile element systematics of (a) Etendeka and (b) West Greenland samples. Stippled lines in (a) and (b) are for two different models. Shown in grey lines in (a) is a model for fractionation of a parental melt with MgO = 13 wt. %, like that expected from >10 % partial melting of a fertile mantle source. This model illustrates that the generally lower MgO northern Etendeka lavas have experienced greater olivine + sulfide fractionation than the southern Etendeka samples. Shown in red lines in (b) is a partial melting model of a primitive mantle source producing initial melt with ~20 wt. % MgO and fractional crystallization to 9.5 wt. % MgO. This model indicates that the high-MgO West Greenland and southern Etendeka samples approximate the composition of partial melting of a peridotite mantle source. Model parameters are given in *Table S3* and normalizations are from Day et al. (2017).

mantle melts (cf., Ordlingassoq versus Naujánguit or Anaanaa Members). The limited range in Os isotope compositions ($\gamma Os_i = +1 \pm 1.6$, 1 St Dev) and the HSE compositions of West Greenland picrites indicate that they are large-degree melts from a peridotitic mantle source, similar to Etendeka picrites.

4.3. Primitive mantle high-$^3He/^4He$ sources during Atlantic Ocean opening

The role that mantle plumes play in the break-up of continents is debated, with arguments for both *active* (e.g., Storey 1995) or *passive* roles during rifting (e.g., Buiter and Torsvik, 2014; Peace et al., 2020; Prasanth et al., 2022). Petrological studies and our HSE and REE modelling indicate that Etendeka and West Greenland picrites derive from high degrees (>16–20 %) of partial melting of peridotite due to high mantle potential temperatures at the base of the lithosphere during their formation (e.g., Larsen and Pedersen, 2000; 2009; Thompson and Gibson, 2000). On the other hand, broader-scale analyses of LIP petrogenesis might suggest that West Greenland and Etendeka picrites are anomalous, and that moderate to ambient temperatures of melting were prevalent in the ~60 Ma NAIP, ~201 Ma Central Atlantic Magmatic Province, and ~132 Ma Paraná-Etendeka CFB, as a whole (e.g., Whalen et al., 2015; Prasanth et al., 2022). Recent studies have argued that lithospheric thinning in response to plate tectonic reconfiguration is what drove continental rifting, leaving a passive role for upwelling mantle and mantle plumes (e.g., Buiter and Torsvik, 2014; Prasanth

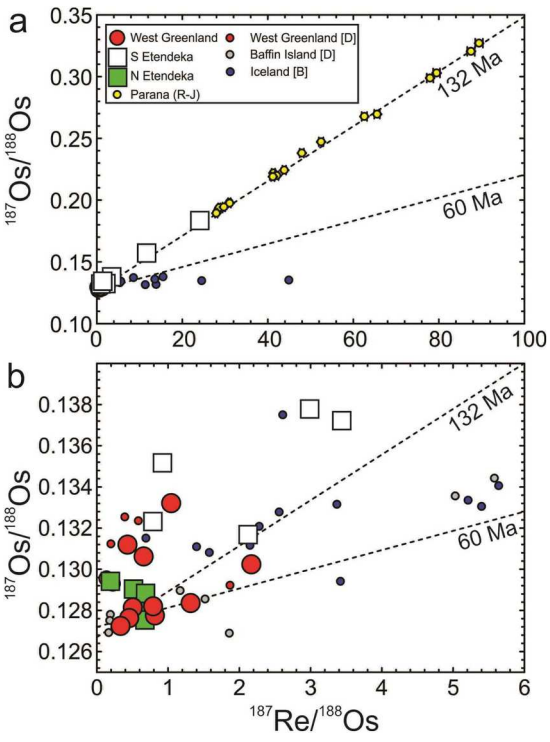

Fig. 5. Diagrams showing (a) full range of $^{187}Re/^{188}Os$ and $^{187}Os/^{188}Os$ for West Greenland and Etendeka samples from this study (large circles) with data for Paraná ([R-J] Rocha-Junior et al., 2012), Baffin Island and West Greenland (without HSE abundances, [D] Dale et al., 2009) and Iceland ([B] Brandon et al., 2007) shown as smaller symbols; (b) restricted range of $^{187}Re/^{188}Os$ (1 to 6) and $^{187}Os/^{188}Os$ for high MgO lavas. Errors are generally smaller than symbols. Dashed isochron reference lines are anchored to chondritic $^{187}Os/^{188}Os$ at 132 Ma and 60 Ma.

et al., 2022). No single scenario of rifting and breakup is likely to fit every LIP, although a key factor can be the buoyancy force and thermal weakening associated with deep-seated mantle plumes, so it is important to establish their presence (e.g., Koptev and Cloetingh, 2024).

As demonstrated in this work, early erupted picritic magmas like those of Etendeka and West Greenland, represent melts from the highest degrees of partial melting experienced in LIP since the Archean (see for example Waterton et al., 2021). As such, even if these melts may be rare in some LIP sequences (they are not rare in West Greenland, nor do they always erupt early in the eruptive sequence), their primitive geochemical signatures are significant for understanding mantle source compositions feeding magmatism. For Etendeka and West Greenland, HSE abundances and Os isotope compositions demonstrate that the primary melts to these rocks originated from melting of peridotite with PM-like HSE characteristics. These same samples are associated with high-$^{3}He/^{4}He$ (Graham et al., 1998; Stuart et al., 2003; Starkey et al., 2009; Stroncik et al., 2017). Furthermore, it is notable that the chondritic to initially modestly supra-chondritic $^{187}Os/^{188}Os$ (i.e., γOs_i a few percent above zero), PM-like HSE contents and high-$^{3}He/^{4}He$ are associated with depleted Sr-Nd-Pb isotope characteristics for the same samples (e.g., Larsen and Pedersen, 2009). These collective isotopic signatures suggest that the depleted high-$^{3}He/^{4}He$ component corresponds to a peridotite source for both West Greenland and the Paraná-Etendeka LIP. This would further indicate that this mantle component has chondrite-relative HSE abundances, including long-term chondritic Re/Os evolution. It follows that depleted mantle components with high-$^{3}He/^{4}He$ that are non-chondritic with respect to lithophile incompatible trace elements likely experienced late-accretion and have chondritic-relative abundances with respect to the HSE.

In detail, the He-isotope data from West Greenland (16.4 to 47.6R_A; Graham et al., 1998; Starkey et al., 2009) and Baffin Island picrites (14.5 to 67R_A; Stuart et al., 2003; Starkey et al., 2009; Horton et al., 2023) all have values higher than MORB (8 ± 2R_A), whereas Etendeka picrites and basalts have a range extending to radiogenic values (1.2 to 25.9R_A; Stroncik et al., 2017). These differences reflect aging and addition of radiogenic ^{4}He to ~132 Ma Etendeka samples (Stroncik et al., 2017), as well as different modes of crustal assimilation and concomitant degassing of He. In the case of northern Etendeka samples, there is a negative relationship between $^{206}Pb/^{204}Pb$ and γOs_i, illustrated by the arrow in Fig. 6, that also covaries with decreasing $^{3}He/^{4}He$, suggesting concomitant degassing with crustal assimilation. For the southern Etendeka dykes, more radiogenic $^{206}Pb/^{204}Pb$ crustal sources appear to play a role in the assimilation, which is consistent with contrasting basement lithologies (more felsic Damara Belt crust in the south and mafic-intermediate Kaoko Belt crust in the northern Etendeka; e.g., Thompson et al., 2007). Contrastingly, West Greenland picrites have a limited range in both He and Pb isotope compositions. These variations in He-Os-Pb isotopes suggest that the samples studied here experienced different extents of modification, but still record signatures of less degassed mantle sources.

Compared with other LIP that have been shown to have CLM, crustal and/or recycled oceanic crustal contributions, the NAIP (West Greenland and Baffin Island) and Etendeka basalts and picrites display a remarkably limited range of Os isotope compositions in Os-Nd isotope space (Fig. 7). Variations in Os and Nd isotopes for Karoo (Ellam et al., 1992; Heinonen et al., 2014), Siberian (Horan et al., 1995) and Emeishan picrites and basalts (Li et al., 2010) have been attributed to assimilation or sourcing of melts from the CLM, or even mantle-derived pyroxenite sources (e.g., Heinonen et al., 2014). The necessary HSE abundance data for these locations are lacking to compare with the NAIP or Etendeka to understand partial melting and later fractionation processes more fully. It is also clear that not all LIP lavas will retain primary mantle characteristics; for example, CLM contributions or ancient oceanic lithosphere are present in some NAIP lavas (Larsen et al., 2003; Peate et al., 2003). Despite evidence for crustal contamination and CLM influences in other LIP, or even within erupted lavas from the same LIP, the high HSE contents and primitive mantle Os isotopic compositions of the NAIP or Etendeka samples suggest they were not affected by these processes. This underscores the relative resistance of the high-Os parent melts to these samples being affected by crustal or CLM assimilation, and

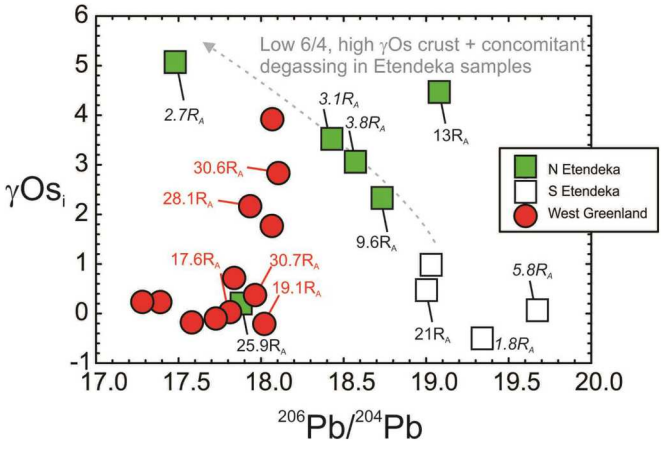

Fig. 6. $^{206}Pb/^{204}Pb$ versus γOs_i ($[(^{187}Os/^{188}Os_{sample}t/^{187}Os/^{188}Os_{chondrites}t)-1] \times 100$) for Etendeka and West Greenland picrites. Numbers at data points show R_A values for He isotope compositions of olivine measured for the samples, from Graham et al. (1998), Starkey et al. (2009) and Stroncik et al. (2017). Lead isotope data for West Greenland from Larsen & Pedersen (2009). The arrow shows the vector for assimilation of low $^{206}Pb/^{204}Pb$ (6/4) crustal components with concomitant degassing of He to explain the variation of Pb, Os and He isotopes for the northern Etendeka samples.

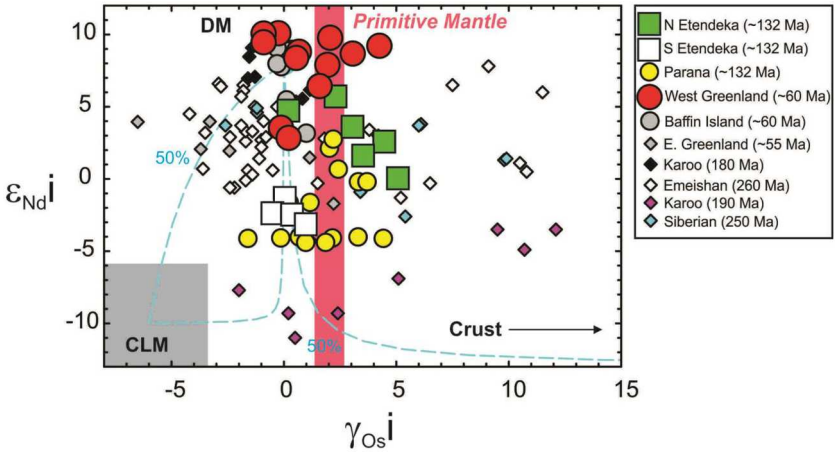

Fig. 7. Initial Os and Nd isotope compositions for West Greenland, Etendeka and Paraná dykes and lavas (Paraná data from Rocha-Junior et al., 2012) versus data for Baffin Island, Emeishan, Siberian and Karoo CFB. Field of CLM is taken from Horan et al. (1995), with CFB data from Horan et al. (1995), Schaefer et al. (2000), Peate et al. (2003), Li et al. (2010) and Heinonen et al. (2014). Also shown are approximate compositions of depleted mantle (DM) and crust from Day (2013). It should be noted that the Os contents of samples plotted from the NAIP, and Etendeka are generally >1 ng/g. For the Karoo, only two samples at ~−2 and +5 γOs_i have >1 ng/g Os. Model parameters are given in *Table S3* for the models of mixing between a primitive melt component similar to West Greenland or Baffin Island picrites and CLM or crust, with PM value for Os isotopes from Day et al. (2017). Blue dashed lines are mixtures between the mantle-derived partial melt and crust or CLM, with the two lines to CLM denoting different initial Os contents in the melt. West Greenland, Baffin Island and Paraná-Etendeka samples do not preserve evidence for significant crustal or CLM contributions to Os isotopes.

their value in assessing mantle source characteristics during continental break-up.

Continental break-up to form the Atlantic Ocean occurred in a piecemeal fashion and is associated with inception of at least three LIP (Paraná-Etendeka, NAIP, CAMP; Fig. 1). Helium isotope data have not been reported for primitive CAMP rocks, but Os isotope data for basaltic rocks associated with CAMP yield initial $^{187}Os/^{188}Os$ slightly higher than PM (errorchron initial $^{187}Os/^{188}Os$ of 0.1298 ± 0.0056 at 200 Ma [$\gamma Os_i = +2.8$]; Callegaro et al., 2014). Peridotite mantle sources with chondritic Re/Os have therefore repeatedly fed LIP magmatism associated with opening of the Atlantic Ocean since ~200 Ma. The He-isotope composition of Etendeka and NAIP magmatism indicates that, at least over a 70 Myr time span (~130 to 60 Ma) a mantle source in both the south and north Atlantic was less-degassed mantle tapped by plumes. Perhaps more remarkably, the compositions of picrites erupted across nearly 60 Myr of evolution within the NAIP suggest that a source with chondritic Re/Os, PM-like HSE abundances and high-$^3He/^4He$ has continued to feed magmatism to this day. Not only do primitive Palaeogene magmas from the British Tertiary Igneous Province ($\gamma Os_i = +2.6$; e.g., O'Driscoll et al., 2009) have similar PM-like HSE characteristics, but modern Icelandic picrites are also characterized by high-$^3He/^4He$ and Os isotope compositions ranging from chondritic to modestly supra-chondritic (Brandon et al., 2007; Nicklas et al., 2021).

The geochemical evidence of plume magmatism related to the Atlantic LIP favours an active rather than a passive role of mantle plumes in continental break-up. In the passive model of top-driven upwelling related to lithospheric rifting, any lower mantle material with the high-$^3He/^4He$ and PM-like HSE compositions of Etendeka and NAIP picrites would likely undergo significant mixing with more degassed, depleted upper mantle components. This scenario is inconsistent with a lack of geochemical evidence for mixing with DM in high-$^3He/^4He$ picrites (e.g., Graham et al., 1998; Schaefer et al., 2000; Starkey et al., 2009; Dale et al., 2009; Stroncik et al., 2017; this study). The Atlantic LIP studied here are therefore in stark contrast with the low-$^3He/^4He$ and moderately sub-chondritic Os isotope compositions of Karoo and Ferrar LIP samples that formed during rifting of Gondwana, separating Africa from Antarctica at ~180 Ma (Heinonen et al., 2014; Heinonen and Kurz, 2015), some 40 Ma prior to south Atlantic rifting.

Additional support for active rifting in response to mantle plumes to form the Atlantic Ocean come from seismic studies of the modern mantle that show evidence for pronounced plume structures rising from the lowermost mantle (e.g., Yuan and Romanowicz, 2017). These plumes have been suggested as the cause of high-$^3He/^4He$ sources (e.g., Stuart et al., 2003; Graham et al., 1998; Horton et al., 2023). From a He isotope perspective, contributions from deep mantle components have been considered to be limited (e.g., Marty and Gezahegn, 1996; Starkey et al., 2009), but from an Os isotope perspective, non-DM contributions appear to be volumetrically significant, at least within Atlantic LIP. The "active" model enables less-degassed peridotite to rise with limited entrainment and mixing with DM. Both Etendeka and NAIP picrites were erupted early in the formation of both LIP and they provide evidence for an active role for mantle plumes in continental break-up along the Atlantic margins.

4.4. Implications for modern high-$^3He/^4He$ ocean island basalts

Atlantic Ocean basin formation was associated with upwelling of less-degassed lower mantle from at least 132 Ma to the present-day and is associated with the highest-$^3He/^4He$ ever measured in volcanic rocks. From a global compilation of volcanic and intrusive rocks, only a select group of samples exist with $^3He/^4He$ ratios within the range of the highest measured in LIP of West Greenland, Baffin Island or the Etendeka (>25R_A; $^4He/^3He$ = <30,000). These are Miocene and recent Icelandic lavas (e.g., Hilton et al., 1999; Macpherson et al., 2005), Loihi Seamount, Hawaii (e.g., Valbracht et al., 1997), Fernandina in the Galapagos archipelago (Kurz et al., 2009) and Ofu in Samoa (Jackson et al., 2009). Loihi, Fernandina and Ofu are also unusual within their respective archipelagos in that most magmatic products otherwise have $^3He/^4He$ <25R_A (e.g., Day et al., 2022a), and similar differences are also observed in LIP like the NAIP with high $^3He/^4He$. A characteristic of the NAIP and Etendeka samples is that high-$^3He/^4He$ ratios are related to chondritic to modestly supra-chondritic (PM-like) Os isotope compositions. Similar compositions are evident for Samoan OIB lavas (Fig. 8) but in contrast, Iceland picrites and lavas from Fernandina and Hawaii extend to more radiogenic Os isotopes for a given He isotopic ratio.

Samoan magmas have been shown to be variably affected by limited quantities of sediment in their mantle source, which is not evident in their Os isotope compositions, consistent with a dominant peridotite mantle source (Jackson and Shirey, 2012). Isotopic compositions of lavas from Fernandina, Hawaii (Loa Trend) and Iceland have been

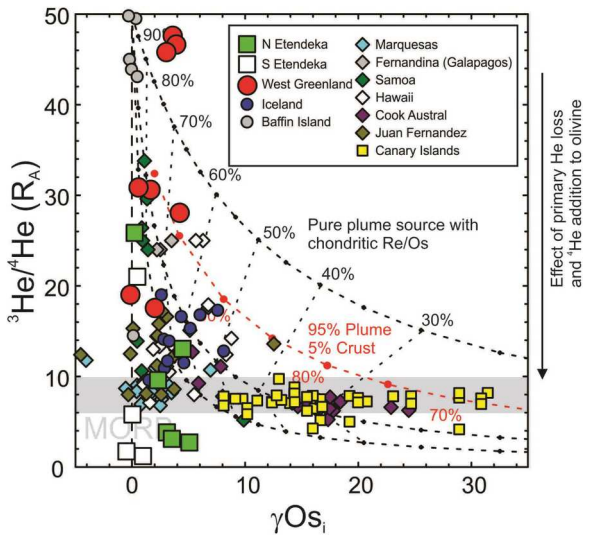

Fig. 8. Plot of $^{3}He/^{4}He$, determined primarily from olivine separates, versus γOs_i in Etendeka, West Greenland and Iceland high-MgO basalts (circle symbols) from this study, Brandon et al. (2007), Starkey et al. (2009) and Dale et al. (2009) versus bulk rocks with >50 pg/g Os for different OIB (diamond or square symbols). Grey horizontal band denotes the MORB range in He isotopes. Full OIB reference data are given in the *Supplementary Information*. Model curves show mixing between 'pure plume source with chondritic Re/Os' (black lines), with three different [He] values between the plume source and crust (top most 1:5, 1:50, 1:100 – in all cases the crustal endmember has the appearance of having higher total [He] than the plume source), and the example of a mixed 95 % Plume, 5 % recycled crust component source with He abundances of 1:5 (red lines). It should be noted that model curves might also extend from suprachondritic values of Os, similar to high-$^{3}He/^{4}He$ West Greenland picrites. Furthermore, mixing is simplified between mantle plume components and crust, with other mantle reservoirs likely to contribute to lava compositions. Model parameters provided in the text and *Table S3*. Note, the effect of primary He loss and ^{4}He addition in olivine is shown as a downward vector on the right-hand side.

explained by mixing between: (1) a lower mantle component, isolated since ~4.5 billion years based on noble gas and W isotope systematics (Mundl et al., 2017), and; (2) ancient recycled oceanic crust, from Sr-Nd-Os-Pb and Xe isotope systematics (e.g., Day et al., 2022a). Osmium isotope ratios that are more radiogenic than present-day chondritic compositions in high-$^{3}He/^{4}He$ OIB such as from Galapagos, Iceland and Hawaii, can be explained by addition of radiogenic Os from subducted components mixed with a depleted high-$^{3}He/^{4}He$ component (e.g., Brandon et al., 2007; Ireland et al., 2009; Gibson et al., 2016). Consequently, of the four OIB localities with high-$^{3}He/^{4}He$ (>25R_A) today, all have parental melts with recycled crustal or lithospheric components.

The degree of partial melting to produce basaltic rocks is essential for understanding the relationship of high-$^{3}He/^{4}He$ with Os isotope systematics. Partial melting to form picrites from this study are estimated to be ~20 % from the HSE and REE, intermediate between the extremely high partial melting extents of Archaean komatiites (40 ± 10 %; Herzberg et al., 1992) and typical estimates of partial melting to produce OIB (typically, 2–10 %; Day et al., 2022b). Differences in partial melting extents are supported by generally more fractionated and lower HSE contents of Hawaiian and Icelandic picrites (e.g., Ireland et al., 2009; Nicklas et al., 2021). During higher degrees of partial melting of a predominantly peridotite source containing recycled components, there would be significant dilution of high Re/Os components. For example, ~20 % partial melting of a peridotite source with chondritic Os but with a 5 % recycled crustal component (0.05 ng/g Os, $^{187}Os/^{188}Os$ = 1) embedded within it produces melts akin to parental melt estimates for Etendeka and West Greenland picrites. On the other hand, 5 % partial melting of an identical source would lead to a more radiogenic composition depending on the fusibility of the recycled crustal component (a 50:50 mixture of components, for example, would lead to a melt with $^{187}Os/^{188}Os$ >0.14 e.g., Day, 2013).

Estimating the isotopic compositions of He in mantle partial melts is more difficult than for Os due to the lack of knowledge regarding He concentrations and the highest-$^{3}He/^{4}He$ in the present-day Earth. While $^{3}He/^{4}He$ as high as the Solar wind (~290R_A) or Jupiter atmosphere composition (~125R_A) have both been proposed for the Earth (see discussion in Day et al., 2022a), we use the maximum value measured in terrestrial rocks as the starting value (50 up to 67R_A; Stuart et al., 2003; Horton et al., 2023). Shown in Fig. 8 are simplified models representing mixing solely between a high-$^{3}He/^{4}He$ mantle source (50R_A in our models) with chondritic Os and a recycled crustal component with low-$^{3}He/^{4}He$ (0.1R_A) and variable He content. The most successful models to explain the Etendeka, West Greenland and Baffin Island picrite data indicate that the radiogenic component has higher He contents than the high-$^{3}He/^{4}He$ mantle source. This is at least partly due to the reliance on He isotope measurements of olivine. If the olivine grains do not faithfully preserve the absolute gas contents of their parental melts then degassing of primary He and addition of ^{4}He would drive their $^{3}He/^{4}He$ ratios down, explaining some of the variability seen in helium isotopes in OIB and LIP. On the other hand, recycled crust components can potentially have high ^{4}He gas contents due to elevated U and Th abundances (e.g., Day et al., 2022a). For example, mantle sources with chondritic Os isotope compositions with 2 %, 5 % or 10 % recycled crust components would have γOs from +0.2 to +1.3, and 45 to 49R_A assuming equal He contents in crust and mantle components. If the crustal component had 5 or 10 times higher relative gas content, this would change the $^{3}He/^{4}He$ to 45 to 32R_A or 41 to 24R_A respectively, with no change in Os isotope composition (*Table S3*). Such large differences in gas content would reflect the ingrowth of ^{4}He in crustal reservoirs. A model for partial melting of a source with 5 % recycled crustal component and 5:1 gas content is shown in red on Fig. 8, illustrating the potential importance of recycled components. In the absence of secular changes in high-$^{3}He/^{4}He$ sources, lower degrees of partial melting and the presence of recycled components can potentially explain the generally lower $^{3}He/^{4}He$ ratios measured for modern lavas today (maximum reported values e.g., Iceland = 34.3R_A, Macpherson et al., 2005; Loihi = 35.3R_A, Valbracht et al., 1997; Ofu = 33.8R_A, Jackson et al., 2009; Fernandina = 30.3R_A, Kurz et al., 2009) relative to 60 Ma NAIP picrites (up to 67R_A).

Recognizing that the degree of partial melting imparts distinct differences between OIB and LIP lavas has several implications. In the first instance, instead of He isotopes being decoupled from other isotopic signatures (e.g., Dale et al., 2009), their variations may reflect the greater influence of recycled components at lower degrees of partial melting. Secondly, relationships between noble gases (He isotopes) and siderophile elements (e.g., Os, W isotopes) are likely to be strongly affected by partial melting processes, especially in OIB. Critically relevant to Atlantic Ocean opening, bursts of deep, plume-derived magmatism associated with the CAMP, Paraná-Etendeka and NAIP LIP were succeeded by more passive upwelling with melting of depleted upper mantle during seafloor spreading along the Mid-Atlantic ridge (Peace et al., 2020). This suggests that, while plume magmatism persists today at Iceland, the main pulses of plume impingement were active drivers of the separation of North and South America from Eurasia and Africa, respectively.

5. Conclusions

Osmium isotope and highly siderophile element abundance systematics of high-$^{3}He/^{4}He$ (>25 R_A) basalts and picrites from the ~132 Ma Etendeka and ~60 Ma NAIP LIP show that mantle sources with chondritic to moderately supra-chondritic $^{187}Os/^{188}Os$ were involved in their petrogenesis. From limited available data, similar deep mantle sources

also appear likely for ~201 Ma CAMP magmas (Callegaro et al., 2014), indicating that deep mantle components were repeatedly involved during continental break up along the entire Atlantic Ocean basin. The presence of high-$^3He/^4He$ components in high degree partial melts without evidence for mixing with DM indicates that this deep mantle signature was associated with plumes that played an *active* rather than a *passive* role in continental rifting. The geochemical evidence of mantle plume contributions to Atlantic LIP should be considered in models of continental break-up and for understanding the role of mantle plumes in Earth surface processes.

The only modern locations with high-$^3He/^4He$ ($>25R_A$) are OIB from the islands of Ofu (Samoa), Loihi seamount (Hawaii) and Fernandina (Galapagos) in the Pacific Ocean, and from Iceland, which is commonly considered the modern manifestation of the NAIP. Unlike high degree partial melts from the Etendeka and NAIP picrites, however, these modern OIB have isotope compositions reflective of recycled oceanic or continental crust within their mantle sources. The extent of partial melting plays a critical role in this contrast of LIP and OIB signatures. The association of high-$^3He/^4He$ with chondritic to modestly supra-chondritic Os isotope compositions in LIP picrites is consistent with high degrees of melting. In lower-degree partial melts like modern OIB, recycled crustal components can dilute high-$^3He/^4He$ signatures and this effect should be considered in geochemical models explaining modern plume magmatism.

CRediT authorship contribution statement

James M.D. Day: Writing – original draft, Resources, Project administration, Methodology, Investigation, Funding acquisition, Formal analysis, Conceptualization. **Sarah J. Woodland:** Writing – review & editing, Methodology, Investigation, Formal analysis, Data curation. **Kimberley L. Nutt:** Writing – review & editing, Investigation, Formal analysis, Data curation. **Nicole Stroncik:** Writing – review & editing, Resources, Data curation. **Lotte M. Larsen:** Writing – review & editing, Validation, Resources. **Robert B. Trumbull:** Writing – review & editing, Validation, Resources, Investigation. **D. Graham Pearson:** Writing – review & editing, Supervision, Methodology, Investigation, Funding acquisition, Formal analysis, Data curation.

Declaration of competing interest

The authors declare no conflicts of interest.

Data availability

Data will be made available on request and are in the tables accompanying this article.

Acknowledgements

This study was supported by a National Science Foundation grant (EAR-1918322) to JMDD. We are grateful to four anonymous reviewers for thought-provoking comments that led to improvement of the manuscript.

Supplementary materials

Supplementary material associated with this article can be found, in the online version, at doi:10.1016/j.epsl.2024.118768.

References

Brandon, A.D., Graham, D.W., Waight, T., Gautason, B., 2007. ^{186}Os and ^{187}Os enrichments and high-$^3He/^4He$ sources in the Earth's mantle: evidence from Icelandic picrites. Geochim. Cosmochim. Acta 71, 4570–4591.

Buiter, S.J., Torsvik, T.H., 2014. A review of Wilson Cycle plate margins: a role for mantle plumes in continental break-up along sutures? Gondwana Res. 26, 627–653.

Callegaro, S., Rapaille, C., Marzoli, A., Bertrand, H., Chiaradia, M., Reisberg, L., Bellieni, G., Martins, L., Madeira, J., Mata, J., Youbi, N., 2014. Enriched mantle source for the Central Atlantic Magmatic Province: new supporting evidence from southwestern Europe. Lithos. 188, 15–32.

Carlson, R.W., 2005. Application of the Pt-Re-Os isotopic systems to mantle geochemistry and geochronology. Lithos. 82, 249–272.

Cheng, Z., Hou, T., Keiding, J.K., Veksler, I.V., Kamenetsky, V.S., Hornschu, M., Trumbull, R.B., 2019. Comparative geothermometry in high-Mg magmas from the Etendeka Province and constraints on their mantle source. J. Petrol. 60, 2509–2528.

Courtillot, V., Jaupart, C., Manighetti, I., Tapponnier, P., Besse, J., 1999. On causal links between flood basalts and continental breakup. Earth Planet. Sci. Lett. 166, 177–195.

Dale, C.W., Pearson, D.G., Starkey, N.A., Stuart, F.M., Ellam, R.M., Larsen, L.M., Fitton, J. G., Macpherson, C.G., 2009. Osmium isotopes in Baffin Island and West Greenland picrites: implications for the $^{187}Os/^{188}Os$ composition of the convecting mantle and the nature of the high $^3He/^4He$ mantle. Earth Planet. Sci. Lett. 278, 267–277.

Day, J.M.D., 2013. Hotspot volcanism and highly siderophile elements. Chem. Geol. 341, 50–74.

Day, J.M.D., 2016. Evidence against an ancient non-chondritic mantle source for North Atlantic igneous province lavas. Chem. Geol. 440, 91–100.

Day, J.M.D., Pearson, D.G., Hulbert, L.J., 2013. Highly siderophile element behaviour during flood basalt genesis and evidence for melts from intrusive chromitite formation in the Mackenzie large igneous province. Lithos. 182-183, 242–258.

Day, J.M.D., Walker, R.J., Warren, J.M., 2017. ^{186}Os-^{187}Os and highly siderophile element abundance systematics of the mantle revealed by abyssal peridotites and Os-rich alloys. Geochim. Cosmochim. Acta 200, 232–254.

Day, J.M.D., Nutt, K.L., Mendenhall, B., Peters, B.J., 2021. Temporally variable crustal contributions to primitive mantle-derived Columbia River Basalt Group magmas. Chem. Geol. 572, 120197.

Day, J.M.D., Jones, T.D., Nicklas, R.W., 2022a. Mantle sources of ocean islands basalts revealed from noble gas isotope systematics. Chem. Geol. 587, 120626.

Day, J.M.D., Moynier, F., Ishizuka, O., 2022b. A partial melting control on the Zn isotope composition of basalts. Geochem. Perspect. Lett. 23, 11–16.

Ellam, R.M., Carlson, R.W., Shirey, S.B., 1992. Evidence from Re-Os isotopes for plume-lithosphere mixing in Karoo flood basalt genesis. Nature 359, 718–721.

Gibson, S.A., Dale, C.W., Geist, D.J., Day, J.A., Brügmann, G., Harpp, K.S., 2016. The influence of melt flux and crustal processing on Re–Os isotope systematics of ocean island basalts: constraints from Galápagos. Earth Planet. Sci. Lett., 449, 345–359.

Graham, D.W., Larsen, L.M., Hanan, B.B., Storey, M., Pedersen, A.K., Lupton, J.E., 1998. Helium isotope composition of the early Iceland mantle plume inferred from the Tertiary picrites of West Greenland. Earth Planet. Sci. Lett. 160, 241–255.

Hart, S.R., Hauri, E.H., Oschmann, L.A., Whitehead, J.A., 1992. Mantle plumes and entrainment: isotopic evidence. Science (1979) 256, 517–520.

Heinonen, J.S., Carlson, R.W., Riley, T.R., Luttinen, A.V., Horan, M.F., 2014. Subduction-modified oceanic crust mixed with a depleted mantle reservoir in the sources of the Karoo continental flood basalt province. Earth Planet. Sci. Lett. 394, 229–241.

Heinonen, J.S., Kurz, M.D., 2015. Low-$^3He/^4He$ sublithospheric mantle source for the most magnesian magmas of the Karoo large igneous province. Earth Planet. Sci. Lett. 426, 305–315.

Herzberg, C., 1992. Depth and degree of melting of komatiites. J. Geophys. Res., Solid Earth 97, 4521–4540.

Hilton, D.R., Grönvold, K., Macpherson, C.G., Castillo, P.R., 1999. Extreme $^3He/^4He$ ratios in northwest Iceland: constraining the common component in mantle plumes. Earth Planet. Sci. Lett. 173, 53–60.

Horan, M.F., Walker, R.J., Fedorenko, V.A., Czamanske, G.K., 1995. Osmium and neodymium isotopic constraints on the temporal and spatial evolution of Siberian flood basalt sources. Geochim. Cosmochim. Acta 59, 5159–5168.

Horton, F., Asimow, P.D., Farley, K.A., Curtice, J., Kurz, M.D., Blusztajn, J., Biasi, J.A., Boyes, X.M., 2023. Highest terrestrial $^3He/^4He$ credibly from the core. Nature 623, 90–94.

Ireland, T.J., Walker, R.J., Garcia, M.O., 2009. Highly siderophile element and ^{187}Os isotope systematics of Hawaiian picrites: implications for parental melt composition and source heterogeneity. Chem. Geol. 260, 112–128.

Jackson, M.G., Kurz, M.D., Hart, S.R., 2009. Helium and neon isotopes in phenocrysts from Samoan lavas: evidence for heterogeneity in the terrestrial high $^3He/^4He$ mantle. Earth Planet. Sci. Lett. 287, 519–528.

Jackson, M.G., Shirey, S.B., 2012. Re–Os isotope systematics in Samoan shield lavas and the use of Os-isotopes in olivine phenocrysts to determine primary magmatic compositions. Earth Planet. Sci. Lett. 312, 91–101.

Kopytev, A., Cloetingh, S., 2024. Role of Large Igneous Provinces in continental break-up varying from "Shirker" to "Producer. Communicat.Earth Enrivon. 5, 27. https://doi.org/10.1038/s43247-023-01191-9.

Kurz, M.D., Jenkins, W.J., Hart, S.R., 1982. Helium isotopic systematics of oceanic islands and mantle heterogeneity. Nature 297, 43–47.

Kurz, M.D., Curtice, J., Fornari, D., Geist, D., Moreira, M., 2009. Primitive neon from the center of the Galápagos hotspot. Earth Planet. Sci. Lett. 286, 23–34.

Larsen, L.M., Pedersen, A.K., 2000. Processes in high-Mg, high-T magmas: evidence from olivine, chromite and glass in Palaeogene picrites from West Greenland. J. Petrol. 41, 1071–1098.

Larsen, L.M., Pedersen, A.K., 2009. Petrology of the Paleocene picrites and flood basalts on Disko and Nuussuaq, West Greenland. J. Petrol. 50, 1667–1711.

Larsen, L.M., Pedersen, A.K., Sundvoll, B., Frei, R., 2003. Alkali picrites formed by melting of old metasomatized lithospheric mantle: Manitdlat Member, Vaigat Formation, Palaeocene of West Greenland. J. Petrol. 44, 3–38.

Li, J., Xu, J.F., Suzuki, K., He, B., Xu, Y.G., Ren, Z.Y., 2010. Os, Nd and Sr isotope and trace element geochemistry of the Muli picrites: insights into the mantle source of the Emeishan large igneous province. Lithos. 119, 108–122.
Lu, G., Huismans, R.S., 2021. Melt volume at Atlantic volcanic rifted margins controlled by depth-dependent extension and mantle temperature. Nat. Commun. 12, 3894.
Macpherson, C.G., Hilton, D.R., Day, J.M.D., Lowry, D., Grönvold, K., 2005. High-$^{3}He/^{4}He$, depleted mantle and low-$\delta^{18}O$, recycled oceanic lithosphere in the source of central Iceland magmatism. Earth Planet. Sci. Lett. 233, 411–427.
Marty, B., Gezahegn, Y., 1996. Helium isotopic variations in Ethiopian plume lavas: nature of magmatic sources and limit on lower mantle contribution. Earth Planet. Sci. Lett. 144, 223–237.
Mundl, A., Touboul, M., Jackson, M.G., Day, J.M.D., Kurz, M.D., Lekic, V., Helz, R.T., Walker, R.J., 2017. 182-W isotope heterogeneity in modern ocean island basalts. Science (1979) 356, 66–69.
Mungall, J.E., Brenan, J.M., 2014. Partitioning of platinum-group elements and Au between sulfide liquid and basalt and the origins of mantle-crust fractionation of the chalcophile elements. Geochim. Cosmochim. Acta 125, 265–289.
Nicklas, R.W., Brandon, A.D., Waight, T.E., Puchtel, I.S., Day, J.M.D., 2021. High-precision Pb and Hf isotope and highly siderophile element abundance systematics of high-MgO Icelandic lavas. Chem. Geol. 582, 120436.
O'Driscoll, B., Day, J.M.D., Daly, J.S., Walker, R.J., McDonough, W.F., 2009. Rhenium–osmium isotopes and platinum-group elements in the Rum Layered Suite, Scotland: implications for Cr-spinel seam formation and the composition of the Iceland mantle anomaly. Earth Planet. Sci. Lett. 286, 41–51.
Peace, A.L., Phethean, J.J., Franke, D., Foulger, G.R., Schiffer, C., Welford, J.K., McHone, G., Rocchi, S., Schnabel, M., Doré, A.G., 2020. A review of Pangaea dispersal and Large Igneous Provinces–In search of a causative mechanism. Earth. Sci. Rev. 206, 102902.
Pearson, D.G., Irvine, G.J., Ionov, D.A., Boyd, F.R., Dreibus, G.E., 2004. Re–Os isotope systematics and platinum group element fractionation during mantle melt extraction: a study of massif and xenolith peridotite suites. Chem. Geol. 208, 29–59.
Peate, D.W., Baker, J.A., Blichert-Toft, J., Hilton, D.R., Storey, M., Kent, A.J.R., Brooks, C.K., Hansen, H., Pedersen, A.K., Duncan, R.A., 2003. The Prinsen af Wales Bjerge Formation lavas, East Greenland: the transition from tholeiitic to alkalic magmatism during Palaeogene continental break-up. J. Petrol. 44 (2), 279–304.
Pernet-Fisher, J.F., Day, J.M.D., Howarth, G.H., Ryabov, V.V., Taylor, L.A., 2017. Atmospheric outgassing and native-iron formation during carbonaceous sediment–basalt melt interactions. Earth Planet. Sci. Lett. 460, 201–212.
Peters, B.J., Day, J.M.D., 2017. A geochemical link between plume head and tail volcanism. Geochem. Perspect. Lett 5, 29–34.
Prasanth, M.M., Shellnutt, J.G., Lee, T.Y., 2022. Secular variability of the thermal regimes of continental flood basalts in large igneous provinces since the Late Paleozoic: implications for the supercontinent cycle. Earth. Sci. Rev. 226, 103928.
Renne, P.R., Glen, J.M., Milner, S.C., Duncan, A.R., 1996. Age of Etendeka flood volcanism and associated intrusions in southwestern Africa. Geology. 24, 659–662.
Rocha-Junior, E.R.V., Puchtel, I.S., Marques, L.S., Walker, R.J., Machado, F.B., Nardy, A. J.R., Babinski, M., Figueiredo, A.M.G., 2012. Re-Os isotope and highly siderophile element systematics of the Paraná continental flood basalts (Brazil). In: Earth and Planetary Science Letters, 337-338, pp. 164–173.
Saunders, A.D., Fitton, J.G., Kerr, A.C., Norry, M.J., Kent, R.W., 1997. The North Atlantic igneous province. In: Mahoney, J.J., Coffin, M.F. (Eds.), Large igneous provinces: continental, oceanic and planetary flood volcanism geophysical monograph Vol. 100. American Geophysical Union, pp. 45–93.
Schaefer, B.F., Parkinson, I.J., Hawkesworth, C.J., 2000. Deep mantle plume osmium isotope signature from West Greenland Tertiary picrites. Earth Planet. Sci. Lett. 175, 105–118.
Starkey, N.A., Stuart, F.M., Ellam, R.M., Fitton, J.G., Basu, S., Larsen, L.M., 2009. Helium isotopes in early Iceland plume picrites: constraints on the composition of the high $^{3}He/^{4}He$ mantle. Earth Planet. Sci. Lett. 277, 91–100.
Storey, B.C., 1995. The role of mantle plumes in continental breakup: case histories from Gondwanaland. Nature 377, 301–308.
Stroncik, N.A., Krienitz, M.S., Niedermann, S., Romer, R.L., Harris, C., Trumbull, R.B., Day, J.M.D., 2017. Helium isotope evidence for a deep-seated mantle plume involved in South Atlantic break-up. Geology. 45, 827–830.
Stuart, F.M., Lass-Evans, S., Fitton, J.G., Ellam, R.M., 2003. High $^{3}He/^{4}He$ ratios in picritic basalts from Baffin Island and the role of a mixed reservoir in mantle plumes. Nature 424, 57–59.
Thompson, R.N., Gibson, S.A., 2000. Transient high temperatures in mantle plume heads inferred from magnesian olivines in Phanerozoic picrites. Nature 407, 502–506.
Thompson, R.N., Gibson, S.A., Dickin, A.P., Smith, P.M., 2001. Early Cretaceous basalt and picrite dykes of the southern Etendeka region, NW Namibia: windows into the role of the Tristan mantle plume in Paraná–Etendeka magmatism. J. Petrol. 42, 2049–2081.
Thompson, R.N., Riches, A.J.V., Antoshechkina, P.M., Pearson, D.G., Nowell, G.M., Ottley, C.J., Dickin, A.P., Hards, V.L., Nguno, A.K., Niku-Paavola, V., 2007. Origin of CFB magmatism: multi-tiered intracrustal picrite-rhyolite magmatic plumbing at Spitzkoppe, western Namibia, during early Cretaceous Etendeka magmatism. J. Petrol. 48, 1119–1154.
Valbracht, P.J., Staudacher, T., Malahoff, A., Allegre, C.J., 1997. Noble gas systematics of deep rift zone glasses from Loihi Seamount. Hawaii. Earth Planet. Sci. Lett. 150, 399–411.
Waterton, P., Mungall, J., Pearson, D.G., 2021. The komatiite-mantle platinum-group element paradox. Geochim. Cosmochim. Acta 313, 214–242.
Whalen, L., Gazel, E., Vidito, C., Puffer, J., Bizimis, M., Henika, W., Caddick, M.J., 2015. Supercontinental inheritance and its influence on supercontinent breakup: the Central Atlantic Magmatic Province and the breakup of Gondwana. Geochem., Geophys., Geosyst. 16, 3532–3554.
Yuan, K., Romanowicz, B., 2017. Seismic evidence for partial melting at the root of major hot spot plumes. Science (1979) 357, 393–397.